Dalton Transactions

Accepted Manuscript

ROYAL SOCIETY OF CHEMISTRY

www.rsc.org/dalton

Journal Name

RSCPublishing

ARTICLE

Mechanistic insight into the reactions of hydride transfer *versus* hydrogen atom transfer by a *trans*-dioxoruthenium(VI) complex†

Cite this: DOI: 10.1039/x0xx00000x

Received 00th January 2012,
Accepted 00th January 2012

DOI: 10.1039/x0xx00000x

www.rsc.org/

Sunder N. Dhuri,[a,b] Yong-Min Lee,[a] Mi Sook Seo,[a] Jaeheung Cho,[a] Dattaprasad D. Narulkar,[b] Shunichi Fukuzumi[a,c,*] and Wonwoo Nam[a,*]

A mononuclear high-valent *trans*-dioxoruthenium(VI) complex, *trans*-$[Ru^{VI}(TMC)(O)_2]^{2+}$ (TMC = 1,4,8,11-tetramethyl-1,4,8,11-tetraazacyclotetradecane), was synthesized and characterized by various spectroscopic techniques and X-ray crystallography. Reactivity of the *trans*-$[Ru^{VI}(TMC)(O)_2]^{2+}$ complex was investigated in hydride transfer and hydrogen atom transfer reactions. The mechanism of hydride transfer from dihydronicotinamide adenine dinucleotide (NADH) analogues to *trans*-$[Ru^{VI}(TMC)(O)_2]^{2+}$, which proceeds *via* a proton-coupled electron transfer (PCET), followed by a rapid electron transfer (ET), has been proposed by the observations of a good linear correlation between log rate constants of *trans*-$[Ru^{VI}(TMC)(O)_2]^{2+}$ and *p*-chloranil (Cl_4Q) and a large kinetic isotope effect (KIE) value of 13(1). In the case of the oxidation of alkyl hydrocarbons by the *trans*-$[Ru^{VI}(TMC)(O)_2]^{2+}$ complex, second-order rate constants were dependant on C-H bond dissociation energy (BDE) of substrates, and a large KIE value of 26(2) was obtained in the oxidation of xanthene and deuterated xanthene-d_2 by the *trans*-$[Ru^{VI}(TMC)(O)_2]^{2+}$ complex, indicating that the C-H bond activation of alkyl hydrocarbons proceeds *via* an H-atom abstraction in the rate-determining step.

Introduction

Mononuclear high-valent metal-oxo complexes of heme and non-heme ligands are active oxidants in a wide range of biological and chemical oxidation reactions.[1,2] The non-heme iron(IV)-oxo species exhibit reactivities in the activation of C-H bonds of substrates that usually occurs *via* a hydrogen atom abstraction as the rate-determining step (r.d.s.).[3] Analogous to iron(IV)-oxo complexes, high-valent ruthenium(IV)-oxo species are capable of oxidizing organic substrates with activated C-H bonds by an electron transfer (ET), proton-coupled electron transfer (PCET), hydrogen atom transfer (HAT), hydride transfer (HT) or oxygen atom transfer (OAT) in aqueous and non-aqueous media.[4]

The present scenario in the ruthenium chemistry reveals that ruthenium complexes with different oxidation states play dynamic roles in the water oxidation catalysis (WOC), wherein various mononuclear high-valent ruthenium-oxo intermediates, such as $[Ru^{IV}(O)]^{2+}$, $[Ru^{V}(O)]^{3+}$, $[Ru^{III}(OOH)]^{2+}$, $[Ru^{IV}(O_2)]^{2+}$ and $[Ru^{V}(O_2)]^{3+}$, have been proposed to initiate the O-O formation.[5] Unfortunately, many of these intermediates have yet to be captured and characterized due to their instability in nature. Beyond the field of WOC, however, there has been much demand to develop ruthenium catalysts for the oxidation of biologically and industrially relevant organic substrates.[6]

While a large number of non-heme ruthenium(IV)-oxo complexes have been explored, the enhanced reactivity of the higher oxidation state of ruthenium such as dioxoruthenium(VI) has merited special attention.[7-9] In ruthenium-oxo chemistry, Groves and co-workers have reported the first example of Ru-based biomimetic dioxygenase catalyst and reported a dioxo(tetramesitylporphyrinato)ruthenium(VI), which is an efficient catalyst in an aerobic epoxidation of olefins at ambient temperatures.[10] The reaction of Ru(II)-beomycins with O_2, H_2O_2 or PhIO was subsequently reported by Garnier-Suillerot and coworkers.[11] While Che and co-workers were the pioneers in the chemistry of high-valent dioxoruthenium(VI) species, such as *trans*-$[Ru^{VI}L(O)_2]^{2+}$ where L is tertiary macrocyclic amine (e.g., 1,4,8,11-tetramethyl-1,4,8,11-tetraazacyclotetradecane (TMC), 1,4,8,12-tetramethyl-1,4,8,12-tetraazacyclopentadecane (15-TMC), 1,5,9,13-tetramethyl-1,5,9,13-tetraazacyclohexadecane (16-TMC) and 1,12-dimethyl-3,4:9,10-dibenzo-1,12-diaza-5,8-dioxacyclopentadecane (N_2O_2)),[9a,9b,12] to the best of our knowledge, the reactivity of only two compounds, namely *trans*-$[Ru^{VI}(N_2O_2)(O)_2]^{2+}$ and *trans*-$[Ru^{VI}(TMC)(O)_2]^{2+}$ (**1**; see Scheme 1), has been explored to a large extend in the oxidative reactions of organic and inorganic substrates.[13,14] The oxidation reactions of organic compounds with **1** reported so far are summarized in Scheme 1.[13]

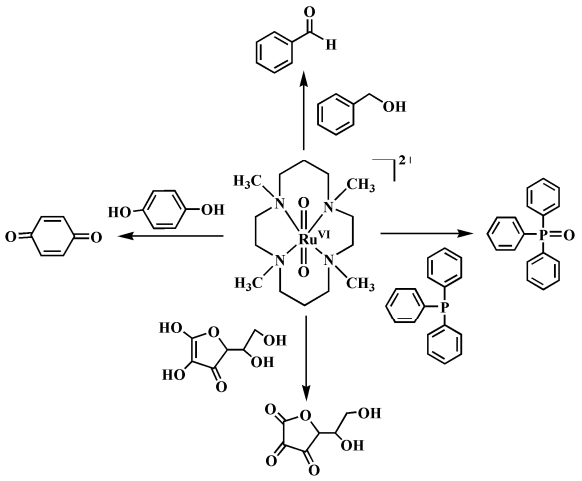

Scheme 1 Chemical structure of **1** and its reactivity in various oxidation reactions.

It is noteworthy that the dioxoruthenium(VI) complexes often react with substrates *via* different mechanisms unlike monooxoruthenium(IV) species. For example, the oxidation of biologically relevant dihydronicotinamide adenine dinucleotide (NADH) analogues by monooxoruthenium(IV) species, *cis*-$[Ru^{IV}(bpy)_2(py)(O)]^{2+}$, was proposed to follow hydrogen atom transfer (HAT) rather than hydride transfer (HT).[15] However, there has been no report on the reactivity of dioxoruthenium(VI) species with the NADH analogues, such as 10-methyl-9,10-dihydroacridine ($AcrH_2$) and its derivatives (see Scheme 2).[16] Although oxidation of NADH follows multiple pathways, it is usually converted to the corresponding cationic form, NAD^+, suggesting a preference of the two-electron and one-proton transfer mechanism of HT.[17]

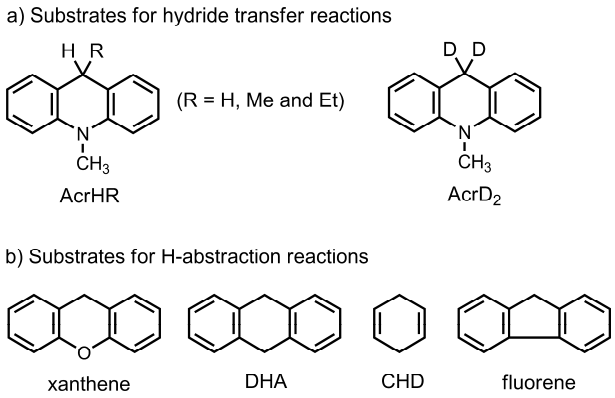

Scheme 2 Substrates used in hydride transfer and hydrogen atom abstraction reactions.

We report herein a detailed characterization of *trans*-$[Ru^{VI}(TMC)(O)_2]^{2+}$ (**1**) by various spectroscopic techniques together with X-ray crystallography and the first example of hydride transfer from NADH analogues to the high-valent dioxoruthenium(VI) complex **1** (see Schemes 1 and 2). In addition, C-H bond activation reactions of alkyl hydrocarbons by **1** were investigated to provide insights into the mechanism that the C-H bond activation reaction proceeds *via* an H-atom abstraction as the rate-determining step.

Results and discussion

Synthesis and characterization of 1.

The *trans*-$[Ru^{VI}(TMC)(O)_2](ClO_4)_2$ (**1**) complex was synthesized according to the literature procedure (see Experimental Section for the detailed synthetic method);[12] **1** is relatively stable in CH_3CN at 0 °C ($t_{1/2} \approx 6$ h). Although UV-vis spectrum of **1** was reported previously,[12] other spectroscopic and structural characterization of **1** has not been reported yet. Thus, we have characterized this complex using various spectroscopic methods, such as ESI-MS, ^1H NMR and EPR, and X-ray crystallography. As shown in Fig. 1a, UV-vis spectrum of **1** exhibits a vibronic band centred at 388 nm, which is characteristic of dioxo-metal complexes.[9a] ESI-MS of **1** exhibits prominent ion peaks at *m/z* = 195.1 and 489.0, whose mass and isotope distribution patterns correspond to $[Ru^{VI}(TMC)(O)_2]^{2+}$ (*calc*. *m/z* = 195.1) and $[Ru^{VI}(TMC)(O)_2(ClO_4)]^+$ (*calc*. *m/z* = 489.1) species, respectively (Fig. 1b). When *trans*-$[Ru^{VI}(TMC)(^{18}O)_2](ClO_4)_2$ (**1**-$^{18}O_2$) was generated using isotopically labelled $H_2{}^{18}O_2$, the mass peak at *m/z* = 489.0 shifts to 493.0, indicating that **1** contains two oxygen atoms. We then investigated an oxygen atom exchange reaction of **1** with isotope labelled water ($H_2{}^{18}O$). Addition of $H_2{}^{18}O$ into a solution of **1** resulted in the disappearance of mass peak at 489.0 due to $[Ru^{VI}(TMC)(^{16}O)_2(ClO_4)]^+$ with the appearance of new mass peaks at *m/z* = 491 and 493, which correspond to

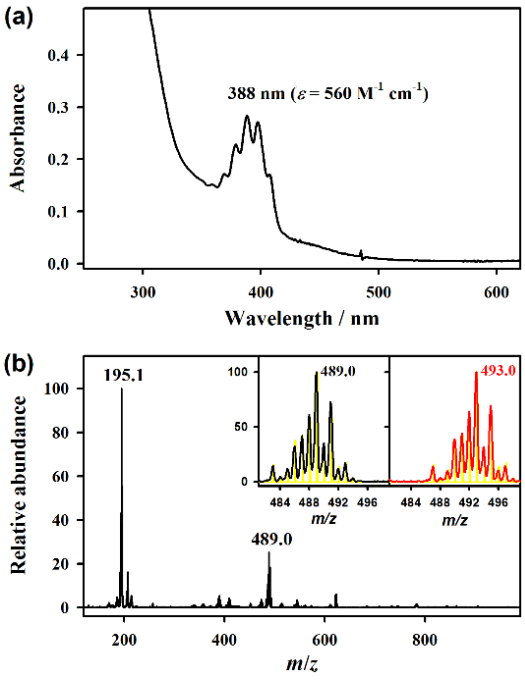

Fig. 1 (a) UV-vis spectrum of *trans*-$[Ru^{VI}(TMC)(O)_2]^{2+}$ (**1**) in CH_3CN at 0 °C. (b) ESI-MS spectrum of **1** in CH_3CN. Insets show the observed (black or red line) and calculated (yellow bar) isotope distribution patterns for **1**-$^{16}O_2$ (left panel) and **1**-$^{18}O_2$ (right panel).

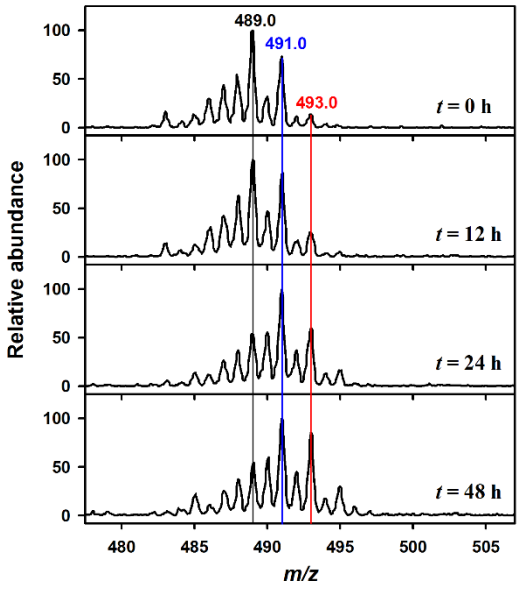

Fig. 2 ESI-MS spectra of the reaction solution obtained upon addition of $H_2{}^{18}O$ (10 μL) into the solution of **1** (1.0 mM) at different time intervals (0 h, 12 h, 24 h and 48 h). The peaks at *m/z* = 489.0, 491.0 and 493.0 correspond to $[Ru^{VI}(TMC)(^{16}O)_2(ClO_4)]^{2+}$ (*calc. m/z* = 489.1), $[Ru^{VI}(TMC)(^{16}O)(^{18}O)(ClO_4)]^{2+}$ (*calc. m/z* = 491.1) and $[Ru^{VI}(TMC)(^{18}O)_2(ClO_4)]^{2+}$ (*calc. m/z* = 493.1), respectively.

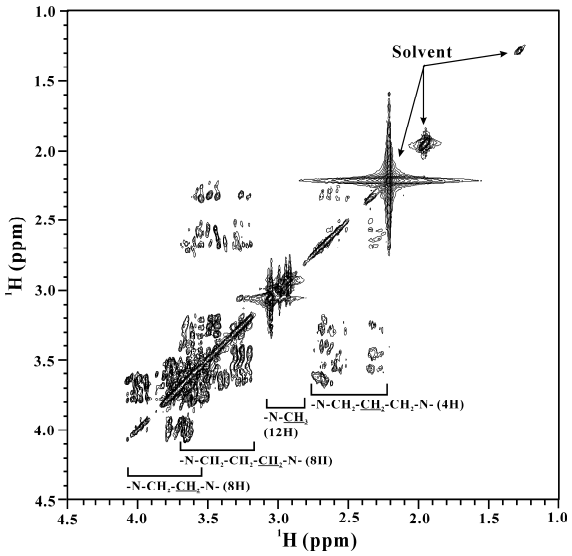

Fig. 3 2D ^1H-^1H-COSY spectrum of **1** in CD_3CN at 25 °C.

$[Ru^{VI}(TMC)(^{16}O)(^{18}O)(ClO_4)]^+$ and $[Ru^{VI}(TMC)(^{18}O)_2(ClO_4)]^+$, respectively (Fig. 2). This result indicates that the two ^{16}O atoms bound to ruthenium(VI) centre exchange with ^{18}O of $H_2{}^{18}O$ in a stepwise manner and the oxygen exchange takes place slowly.[18] The observations that **1** is EPR silent and 2D ^1H-^1H COSY spectrum of **1** exhibits all peaks located in the diamagnetic region (Fig. 3) indicate that **1** is a diamagnetic low-spin ($S = 0$) d^2 Ru^{VI} species. Taken together, all the spectroscopic data demonstrate that **1** is a dioxoruthenium(VI) species.

In addition to the spectroscopic characterization described above, **1** was characterized structurally by X-ray crystallography. The greater thermal stability of **1** allowed the isolation of single crystals suitable for X-ray crystal structural analysis. Although H atoms were not geometrically positioned due to the relatively high degree of disorders, the structure of **1** shows a perfect octahedral geometry with space group $P2_1/c$ (Fig. S1 and Table S1, ESI†). In this structure, one oxo ligand is located *trans* to the other oxo ligand, and two *N*-methyl groups of the TMC ligand point toward one oxo ligand and other two N-methyl groups of the TMC ligand point toward the other oxo ligand symmetrically. Both the *trans* Ru-O bond distances are 1.712(4) Å, which is quite similar to those reported in dioxoruthenium(VI) complexes.[19]

Hydride Transfer (HT) from NADH analogues to 1.

The reactivity of **1** was investigated in HT reactions with NADH analogues, 10-methyl-9,10-dihydroacridine ($AcrH_2$) and its derivatives (see Scheme 2), in CH_3CN at 0 °C. Upon addition of $AcrH_2$ to a solution of **1** (5×10^{-5} M), $AcrH_2$ was converted to 10-methylacridinium ion ($AcrH^+$)[20] quantitatively as evidenced from the full formation of a band at 358 nm ($\varepsilon = 1.8 \times 10^4$ M^{-1} cm^{-1}) due to $AcrH^+$ (Fig. 4a) and metal product was $[Ru^{IV}(TMC)(O)]^{2+}$ (Fig. S2, ESI† for ESI-MS).[21] First-order rate constants (k_{obs}), determined by pseudo-first order fitting of the kinetic data for the formation of $AcrH^+$ monitored at 358 nm, increased linearly with an increase in concentration of $AcrH_2$, leading us to determine the second-order rate constant (k_{HT}) of 63(4) M^{-1} s^{-1} (Fig. 4b; see also Fig. S3a, ESI†). By using dideuterated substrate, $AcrD_2$, a large kinetic isotope effect (KIE) value of 13(1) was determined in the reactions of $AcrH_2$ *versus* $AcrD_2$ (Fig. 4b), indicating that the C-H bond cleavage of NADH analogues is involved in the rate-determining step in the HT reactions by **1**. The HT reactions were also investigated with other $AcrH_2$ derivatives bearing a substituent R at the C-9 position (i.e., AcrHR), such as AcrHMe and AcrHEt. The reaction rates (k_{HT}), which were determined to be 2.7(2) M^{-1} s^{-1} for AcrHMe and 1.3(1) M^{-1} s^{-1} for AcrHEt (Fig. S3, ESI†), were significantly affected by the substituent R in the AcrHR. The observation that reactivity of AcrHR bearing an electron-donating R group is lower than that of $AcrH_2$ suggests that the HT reaction occurs *via* a sequential electron and proton transfer, followed by a rapid ET, rather than an one-step HT mechanism.[22,23] The decrease in the second-order rate constants with the increasing electron-donating ability of R (methyl or ethyl) at the C-9 position rather indicates that the reactivity is determined by the process in which a positive charge is released.[20,22] It should be noted that the reaction of $[Ru^{IV}(TMC)(O)]^{2+}$ with $AcrH_2$, which was performed as a control experiment, does not occur under the identical conditions.

As reported previously, HT from NADH analogues to hydride acceptors, such as *p*-chloranil (Cl_4Q) and 2,3-dichloro-5,6-dicyano-*p*-benzoquinone, occurs *via* a proton-coupled electron transfer (PCET), followed by a rapid ET.[24,25] Further, the reactivity comparison between high-valent metal-oxo

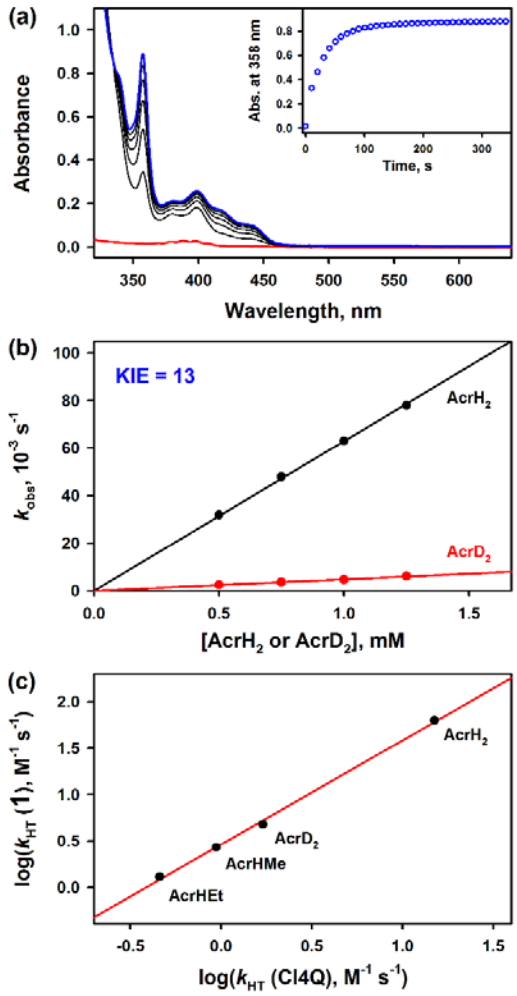

Fig. 4 (a) UV-vis spectral changes of **1** observed in the reaction of **1** (0.050 mM) and $AcrH_2$ (1.0 mM) in CH_3CN at 0 °C. Inset shows time course monitored at 358 nm due to the formation of $AcrH^+$. (b) Plots of k_{obs} against concentrations of $AcrH_2$ and $AcrD_2$. (c) Plot of log k_{HT} for hydride transfer from NADH analogues to **1** in CH_3CN at 0 °C *versus* log k_{HT} for hydride transfer from the same series of NADH analogues to Cl_4Q[22] in CH_3CN at 25 °C.

complexes and Cl_4Q was used as an indirect evidence for proposing the PCET mechanism in HT reactions.[25] Thus, the rate constants of HT (k_{HT}) from NADH analogues to **1** were compared with those of HT from the same NADH analogues to Cl_4Q.[20,25,26] As shown in Fig. 4c, there is a good linear correlation between the k_{HT} values of **1** and the corresponding values of Cl_4Q with the slope of ~1, implying that HT from NADH analogues to **1** follows the same HT mechanism of Cl_4Q, which is the PCET, followed by rapid ET.[24] In addition, the k_{HT} values of HT from NADH analogues to **1** are also well correlated with the rate constants of deprotonation (k_d) of NADH radical cations (i.e., one-electron oxidized product of AcrHR, $AcrHR^{\bullet+}$) as shown in Fig. S4, ESI†. As reported previously, the decay of $AcrHR^{\bullet+}$ obeys first-order kinetics and the decay rate constant of $AcrHR^{\bullet+}$ (k_d) corresponds to the rate constant of deprotonation from $AcrHR^{\bullet+}$ to produce $AcrR^{\bullet}$.[20,22] The k_d value becomes smaller by changing R from H to Me and Et because of an increase in the

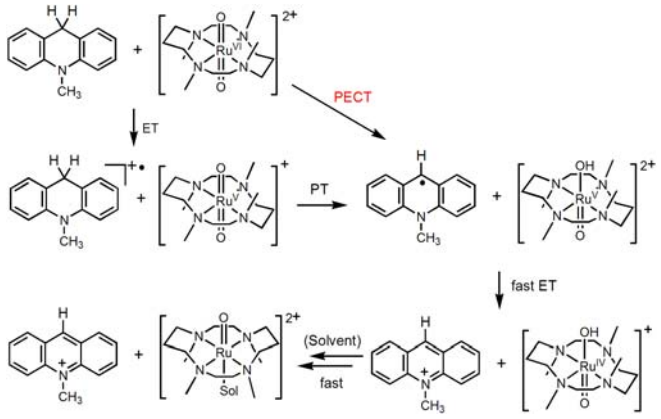

Scheme 3 Proposed mechanism for HT from NADH analogues, AcrHR, to **1**.

deprotonation barrier to form the planar $AcrR^{\bullet}$ caused by the increase in the magnitude of nonplanarity of the acridine ring upon introduction of a substituent R at the C-9 position in $AcrH_2$.[20,22] Therefore, such a linear correlation between the k_{HT} values of HT from NADH analogues to **1** and the k_d values of deprotonation of $AcrHR^{\bullet+}$ (Fig. S4, ESI†) indicates that the proton transfer (PT) from $AcrHR^{\bullet+}$ to $[Ru^V(TMC)(O)_2]^+$, which is one-electron reduced species of **1**, is involved as the rate-determining step.[20,22] Based on the results of the mechanistic studies discussed above, we propose the following mechanism in the HT reactions by **1** (see Scheme 3): The HT from NADH analogues, AcrHR, to **1** occurs *via* an uphill ET from AcrHR to **1**, followed by the rate-limiting PT from $AcrHR^{\bullet+}$ to $[Ru^V(TMC)(O)_2]^+$ in competition with the back electron transfer, and then rapid ET from $AcrR^{\bullet}$ to the $[Ru^V(TMC)(O)(OH)]^{2+}$ species to produce $AcrR^+$, which is an NAD^+ analogue, and the $[Ru^{IV}(TMC)(O)]^{2+}$ complex.

C-H bond activation of alkyl hydrocarbons by 1.

The reactivity of **1** in the oxidation of alkyl hydrocarbons was also investigated. The reactions of **1** with alkyl hydrocarbons having weak C-H bond dissociation energies (BDE),[27] such as xanthene (75.5 kcal mol^{-1}), dihydroanthracene (DHA; 77.0 kcal mol^{-1}), 1,4-cyclohexadiene (CHD; 78.0 kcal mol^{-1}) and fluorene (80.0 kcal mol^{-1}) (see Scheme 2), were carried out in CH_3CN at 35 °C. As shown in Fig. 5a, addition of xanthene to the acetonitrile solution of **1** (0.50 mM) afforded the disappearance of a vibronic structural absorption peak at 388 nm due to **1**, accompanied by a new absorption band formation at 420 nm, which corresponds to $[Ru^{IV}(TMC)(O)(CH_3CN)]^{2+}$,[21] with clean isosbestic points at 345 and 415 nm (Fig. 5a). The formation of $[Ru^{IV}(TMC)(O)(CH_3CN)]^{2+}$ was confirmed by ESI-MS spectroscopy (Fig. 5b); the ESI-MS spectrum of the reaction solution exhibits prominent ion peaks at m/z = 207.5 and 473.0, whose mass and isotope distribution patterns correspond to $[Ru^{IV}(TMC)(O)(CH_3CN)]^{2+}$ (*calc.* m/z = 207.6) and $[Ru^{IV}(TMC)(O)(ClO_4)]^+$ (*calc.* m/z = 473.1), respectively. This was also confirmed by cyclic voltammetry for the reaction of **1** with DHA (Fig. S5, ESI†). First-order rate constants (k_{obs}), determined by pseudo-first-order fitting of the kinetic data for

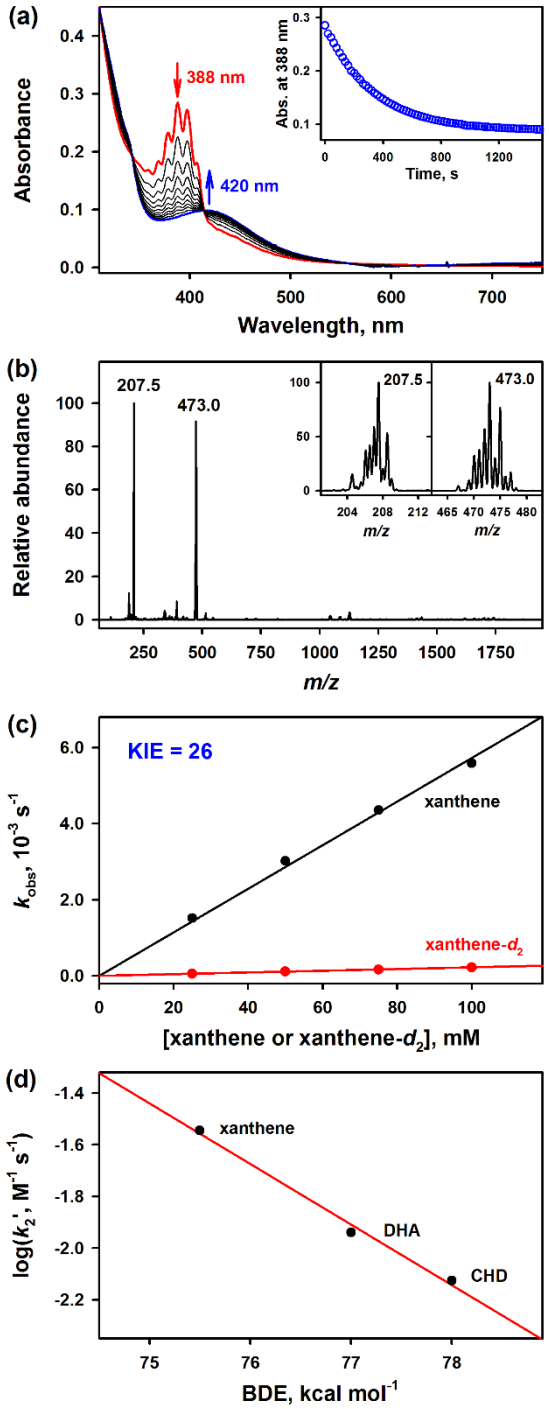

Fig. 5 (a) UV-vis spectral changes of **1** (0.50 mM) upon addition of xanthene (50 mM) at 35 °C. Inset shows time course of the decay of **1** monitored at 388 nm. (b) ESI-MS spectrum of the reaction solution obtained in the reaction of **1** (1.0 mM) with xanthene (50 mM) in CH_3CN at 35 °C. The peaks at m/z = 207.5 and 473.0 correspond to $[Ru^{IV}(TMC)(O)(CH_3CN)]^{2+}$ (*calc.* m/z = 207.6) and $[Ru^{IV}(TMC)(O)(ClO_4)]^{+}$ (*calc.* m/z = 473.1), respectively. Insets show the isotopic distribution patterns of the peaks at m/z = 207.5 and 473.0. (c) Plots of k_{obs} against concentrations of xanthene and xanthene-d_2 to determine the KIE value of 26(2). (c) Plot of log k_2' of **1** against C-H BDE of substrates. Second-order rate constants (k_{HAT}) were determined at 35 °C and then adjusted for reaction stoichiometry to yield k_2' based on the number of equivalent target C-H bonds of substrates (e.g., 2 for xanthene and 4 for DHA and CHD).

the decay of **1** at 388 nm, increased proportionally with the increase of xanthene concentration, leading us to determine the second-order rate constant (k_{HAT}) of 5.7(4) × 10^{-2} M^{-1} s^{-1} at 35 °C (Fig. 5c; see also Fig. S6a, ESI†). It should be noted that, although the reaction product, $[Ru^{IV}(TMC)(O)(CH_3CN)]^{2+}$, reacts further with xanthene,[21] the rate of xanthene oxidation by **1** is 20-fold faster than that of the $[Ru^{IV}(TMC)(O)(CH_3CN)]^{2+}$ reaction with xanthene at the same temperature. In order to determine KIE value, xanthene-d_2 was used as a substrate and the second-order rate constant of 2.2(2) × 10^{-3} M^{-1} s^{-1} was obtained (Fig. 5c), resulting in a large KIE value of 26(2) for the reactions of xanthene *versus* xanthene-d_2 was determined (Fig. 5d). This result indicates that the H-atom abstraction of alkyl hydrocarbons by **1** is involved in the rate-determining step. It should be noted that such a large KIE value in HAT reactions as well as in HT reactions is probably attributed to the tunnelling effects.[4d,4f,4h,7b,9e,15]

The C-H bond activation reactions were also investigated with other alkyl hydrocarbons, such as DHA, CHD and fluorene. The second-order rate constants (k_{HAT}) of 3.6(4) × 10^{-2} and 1.5(2) × 10^{-2} M^{-1} s^{-1} were determined in the reactions of **1** with DHA and CHD, respectively (Fig. S6, ESI†). However, **1** did not show a reactivity with fluorene, which has a relatively strong C-H BDE value (80.0 kcal mol^{-1}) compared to other alkyl hydrocarbons used in this study. As expected, the rate constants (k_{HAT}) decreased with an increase in the C-H BDE of alkyl hydrocarbons. Fig. 5d shows a linear correlation between the log k_2' values and the C-H BDE values of the substrates (the k_{HAT} values are divided by the number of equivalent target C-H bonds of substrates to obtain the k_2' values).[28,29] The final reaction solutions obtained in the oxidation of alkyl hydrocarbons by **1** were analyzed by gas chromatography (GC). Xanthone (87 ± 4%), anthracene (90 ± 4%) and benzene (88 ± 5%) were formed as the major organic products in the oxidation of xanthene, DHA and CHD by **1**, respectively.

The results of the large KIE values, the good correlation between log k_{HAT} and C-H BDE of alkyl hydrocarbons and organic/inorganic product analyses allowed us to propose that the C-H bond activation of alkyl hydrocarbons by **1** occurs *via* an H-atom abstraction mechanism as shown in Scheme 4.

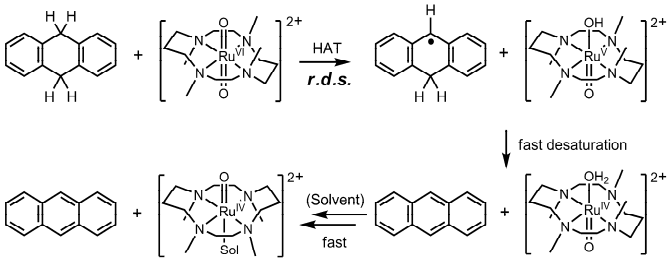

Scheme 4 Proposed mechanism for HAT reaction of DHA by **1**.

Conclusions

In summary, we have synthesized and characterized the mononuclear high-valent *trans*-dioxoruthenium(VI) complex bearing a macrocyclic supporting ligand, *trans*-$[Ru^{VI}(TMC)(O)_2]^{2+}$ (**1**). Reactivities of **1** in HT reactions with NADH analogues and HAT reactions with alkyl hydrocarbons were investigated. On the basis of the reactivity studies, mechanisms of HT from the NADH analogues to **1** and HAT of alkyl hydrocarbons by **1** have been proposed; the HT from NADH analogues, AcrHR, to **1** occurs *via* an uphill ET from AcrHR to **1**, followed by the rate-limiting PT from $AcrHR^{\bullet+}$ to $[Ru^{V}(TMC)(O)_2]^{+}$ species, and then rapid ET from $AcR^{\bullet}$ to the $[Ru^{V}(TMC)(O)(OH)]^{2+}$ species. In the case of the HAT reaction by **1**, the C-H bond activation of alkyl hydrocarbons by **1** occurs *via* an H-atom abstraction mechanism. The mechanistic distinction between NADH analogues and alkyl hydrocarbons may result from the significantly lower one-electron oxidation potentials of NADH analogues than those of alkyl hydrocarbons, which enables the ET pathway.[22-24] Thus, the present work provides valuable insights into the mechanism in the HT and HAT reactions by high-valent dioxoruthenium(VI) species.

Experimental

Materials

Commercially available chemicals were used without further purification unless otherwise indicated. Solvents were distilled under N_2 prior to use according to published procedures.[30] Potassium aquapentachlororuthenate(III) ($K_2[Ru(H_2O)(Cl)_5]$), TMC, xanthene, 9,10-dihydroanthracene, 1,4-cyclohexadiene, $HClO_4$, H_2O_2 (30 %) and $NaClO_4$ were purchased from Aldrich Chemical Co. The isotope labelled $H_2{}^{18}O$ (95 % ^{18}O-atom enriched) and $H_2{}^{18}O_2$ (90 % ^{18}O-enriched, 2 % $H_2{}^{18}O_2$ in $H_2{}^{18}O$) were obtained from ICON Services Inc. (Summit, NJ, USA). The NADH analogues, 10-methyl-9,10-dihydroacridine ($AcrH_2$), 10-methyl-9,10-dideuteroacridine ($AcrD_2$) and 9-Alkyl-10-methyl-9,10-dihydroacridine (AcrHR; R = Me and Et), were prepared by literature methods.[22] The dideuterated substrate xanthene-d_2, was also prepared by literature method.[31] Xanthene (0.50 g, 2.7 mmol) was reacted with NaH (0.20 g, 8.1 mmol) in DMSO-d_6 (3.0 mL) under an inert atmosphere. The deep red solution was stirred at room temperature for 8 h and then quenched with D_2O (5.0 mL). The crude product was filtered and washed with copious amounts of D_2O. ^1H NMR confirmed >99% deuteration. Ruthenium complexes, *trans*-$[Ru^{III}(TMC)Cl_2]Cl$ and $[Ru^{IV}(TMC)(O)(CH_3CN)](ClO_4)_2$ were prepared by the literature method.[9a,32]

Instrumentation

UV-vis spectra and kinetic data were collected on Hewlett Packard Agilent 8453 UV-visible spectrophotometer equipped with an UNISOKU Scientific Instruments or with a circulating water bath. Electrospray ionization mass (ESI-MS) spectra were collected on a Thermo Finnigan (San Jose, CA, USA) LCQ™ Advantage MAX quadrupole ion trap instrument, by infusing samples directly into the source at 20 μL/min using syringe pump. Spray voltage was set at 4.7 kV and while the capillary temperature was maintained at 80 °C. The electron paramagnetic resonance (EPR) spectra were measured using X-band Bruker EMX-plus spectrometer equipped with dual mode cavity (ER 4116DM). Low temperatures were achieved with Oxford Instruments ESR900 liquid He quartz cryostat with Oxford Instruments ITC503 temperature and gas flow controller. The experimental parameters for EPR spectra were as follows: microwave frequency = 9.648 GHz, microwave power = 1.0 mW, modulation amplitude = 10 G, gain = 1 x 10^4, modulation frequency 100 kHz, time constant = 40.96 ms, conversion time = 85.00 ms and measuring temperature = 5 K. ^1H NMR spectra were measured with Bruker model digital AVANCE III 400 FT-NMR spectrometer. Electrochemical measurements (i.e., cyclic voltammetry) were performed on a CH Instrument (CHI630B) electrochemical analyzer in deaerated CH_3CN in the presence of 0.10 M tetra-*n*-butylammonium hexafluorophosphate (Bu_4NPF_6) as a supporting electrolyte. A conventional three-electrode cell was used with a platinum working electrode (surface area of 0.3 mm^2) and a platinum wire as a counter electrode. The platinum working electrodes (BAS) were routinely polished with BAS polishing alumina suspension and rinsed with CH_3CN before use. The measured potentials were recorded as a function of $Ag/AgNO_3$ (0.01 M) reference electrode. All potentials (*vs.* Ag/Ag^+) were converted to values *vs.* SCE by adding 0.29 V.[33] Organic product analysis was carried out using Agilent Technologies 6890N gas chromatograph (GC) and Thermo Finnigan (Austin, Texas, USA) FOCUS DSQ (dual stage quadrupole) mass spectrometer interfaced with Finnigan FOCUS gas chromatograph (GC-MS).

Preparation of *trans*-$[Ru^{VI}(TMC)(O)_2]^{2+}$ (1)

trans-$[Ru^{VI}(TMC)(O)_2]^{2+}$ (**1**) was prepared by literature procedure.[12] Silver *p*-toluenesulfonate (0.54 g, 1.9 mmol) was added to the aqueous solution of *trans*-$[Ru^{III}(TMC)Cl_2]Cl$ (0.30 g, 0.58 mmol) and mixture was warmed on water bath for 30 min. The white precipitates of AgCl formed were filtered and H_2O_2 (30 %, 3.0 mL) was added to the filtrate. The solution was then heated on a water bath until the full formation of a peak at 388 nm in UV-vis spectrum for **1** was observed. The saturated solution (5.0 mL) of $NaClO_4$ was then added to the mixture and kept for cooling in refrigerator. After 2 days, the yellow solid complex with yield of 55 % was formed.

Kinetic measurement and reactivity study

All the reactions were run in a 1-cm quartz cuvette and followed by monitoring the UV-vis spectral changes of the reaction solutions. The rate constants were determined under pseudo-first-order conditions (e.g., [substrate]/[**1**] > 10), by fitting the changes in absorbance for the formation 358 nm peak due to $AcrH^+$ ion in the reaction of **1** with NADH analogues at 0 °C. In the oxidation of alkyl hydrocarbons by **1**, the reactions were monitored by UV-vis spectral changes of the absorption band at 388 nm due to the decay of **1**. First order rate constants were obtained by fitting of the kinetic data at 388 nm. The hydrocarbons with C-H bond dissociation energies (BDE) ranging between 75-80 kcal mol^{-1} were chosen for the reactivity

studies. The reactions were run at least in triplicate, and the data reported here represent the average of these reactions.

Product Analysis

The organic product $AcrH^+$ formed in the reaction of **1** and $AcrH_2$ was quantitatively detected by the absorption band at 358 nm due to $AcrH^+$ ion by UV-vis spectroscopy. The $AcrH^+$ was also detected by ESI-MS spectrum, which showed peak at *m/z* = 194.1 for $AcrH^+$ ion (Fig. S2, ESI†). In the oxidation of xanthene, DHA and CHD by **1**, the complete reaction solutions were analyzed by GC. Product yields were determined by comparing the peak areas with the standard curves obtained using authentic samples and decane as an internal standard. The reaction products for xanthene, DHA and CHD were determined to be xanthone (87 ± 4%), anthracene (90 ± 4%) and benzene (88 ± 5%) as the major organic products, respectively. The ruthenium products formed in the reaction of **1** with $AcrH_2$ as well as alkyl hydrocarbons were analyzed by EPR and ESI-MS techniques. In both reactions, $[Ru^{IV}(TMC)(O)]^{2+}$ species was formed as a final product.[9a,21]

Acknowledgements

The authors gratefully acknowledge research support of this work by the NRF of Korea through CRI (NRF-2012R1A3A2048842 to W.N.) and GRL (NRF-2010-00353 to W.N.), and by an ALCA project from JST, Japan (to S.F). SND acknowledge research support from Department of Science and Technology (DST), New Delhi, India through SR/FT/CS-006/2010 project.

Notes and References

[a] Department of Chemistry and Nano Science, Center for Biomimetic System, Ewha Womans University, Seoul 120-750, Korea. E-mail: wwnam@ewha.ac.kr

[b] Department of Chemistry, Goa University, Goa, 403 206, India.

[c] Department of Material and Life Science, Graduate School of Engineering, ALCA, JST, Osaka University, Suita, Osaka 565-0871, Japan. E-mail: fukuzumi@chem.eng.osaka-u.ac.jp

† Electronic Supplementary Information (ESI) available: [details of any supplementary information available should be included here]. See DOI: 10.1039/b000000x/

1 (a) R. A. Sheldon and J. K. Kochi, *Metal-Catalyzed Oxidations of Organic Compounds*, Academic Press, New York, 1981; (b) B. Meunier, *Biomimetic Oxidations Catalyzed by Transition Metal Complexes*, Imperial College Press, London, 1998; (c) P. R. Ortiz de Montellano, *Cytochrome P450: Structure, Mechanism, and Biochemistry*, 3rd ed., Kluwer Academic / Plenum Publishers, New York, 2005.

2 (a) C. Krebs, D. G. Fujimori, C. T. Walsh and J. M. Bollinger, Jr., *Acc. Chem. Res.,* 2007, **40**, 484-492; (b) J. Hohenberger, K. Ray and K. Meyer, *Nat. Commun.,* 2012, **3**, DOI: 10.1038/ncomms1718; (c) C.-M. Che, V. K.-Y. Lo, C.-Y. Zhou and J.-S. Huang, *Chem. Soc. Rev.*, 2011, **40**, 1950-1975; (d) T. Punniyamurthy, S. Velusamy and J. Iqbal, *Chem. Rev.*, 2005, **105**, 2329-2363; (e) A. S. Borovik, *Chem. Soc. Rev.*, 2011, **40**, 1870-1874; (f) H. Kotani, S. Kaida, T. Ishizuka, M. Sakaguchi, T. Ogura, Y. Shiota, K. Yoshizawa and T. Kojima, *Chem. Sci.*, 2015, **6**, 945-955.

3 (a) W. Nam, Y.-M. Lee and S. Fukuzumi, *Acc. Chem. Res.*, 2014, **47**, 1146-1154; (b) W. Nam, *Acc. Chem. Res.*, 2007, **40**, 522-531; (c) S. P. de Visser, J.-U. Rohde, Y.-M. Lee, J. Cho and W. Nam, *Coord. Chem. Rev.,* 2013, **257**, 381-393; (d) S. Shaik, H. Hirao and D. Kumar, *Acc. Chem. Res.,* 2007, **40**, 532-542; (e) M. T. Green, *Curr. Opin. Chem. Biol.,* 2009, **13**, 84-88; (f) J. Kaizer, E. J. Klinker, N. Y. Oh, J.-U. Rohde, W. J. Song, A. Stubna, J. Kim, E. Münck, W. Nam and L. Que, Jr., *J. Am. Chem. Soc.,* 2004, **126**, 472-473; (g) A. Gunay and K. H. Theopold, *Chem. Rev.*, 2010, **110**, 1060-1081; (h) K. Ray, F. F. Pfaff, B. Wang and W. Nam, *J. Am. Chem. Soc.*, 2014, **136**, 13942-13958.

4 (a) S. A. Trammell, J. C. Wimbish, F. Odobel, L. A. Gallagher, P. M. Narula and T. J. Meyer, *J. Am. Chem. Soc.*, 1998, **120**, 13248-13249; (b) L. K. Stultz, M. H. V. Huynh, R. A. Binstead, M. Curry and T. J. Meyer, *J. Am. Chem. Soc.*, 2000, **122**, 5984-5996; (c) W. K. Seok and T. J. Meyer, *J. Am. Chem. Soc.*, 1988, **110**, 7358-7367; (d) L. Roecker and T. J. Meyer, *J. Am. Chem. Soc.,* 1987, **109**, 746-754; (e) M. S. Thompson and T. J. Meyer, *J. Am. Chem. Soc.*, 1982, **104**, 5070-5076; (f) M. S. Thompson and T. J. Meyer, *J. Am. Chem. Soc.*, 1982, **104**, 4106-4115; (g) W. K. Seok and T. J. Meyer, *Inorg. Chem.*, 2004, **43**, 5205-5215; (h) J. R. Bryant and J. M. Mayer, *J. Am. Chem. Soc.*, 2003, **125**, 10351-10361.

5 (a) I. López, M. Z. Ertem, S. Maji, J. Benet-Buchholz, A. Keidel, U. Kuhlmann, P. Hildebrandt, C. J. Cramer, V. S. Batista and A. Llobet, *Angew. Chem. Int. Ed.*, 2014, **53**, 205-209; (b) J. J. Concepcion, J. W. Jurss, J. L. Templeton and T. J. Meyer, *J. Am. Chem. Soc.*, 2008, **130**, 16462-16463; (c) Z. Chen, J. J. Concepcion, H. Luo, J. F. Hull, A. Paul and T. J. Meyer, *J. Am. Chem. Soc.*, 2010, **132**, 17670-17673; (d) X. Liu and F. Wang, *Coord. Chem. Rev.*, 2012, **256**, 1115-1136; (e) C.-M. Che, V. W.-W. Yam and T. C. W. Mak, *J. Am. Chem. Soc.*, 1990, **112**, 2284-2291; (f) X. Guan, S. L.-F. Chan and C.-M. Che, *Chem. Asian J.*, 2013, **8**, 2046-2056.

6 (a) A. K. Vannucci, J. F. Hull, Z. Chen, R. A. Binstead, J. J. Concepcion and T. J. Meyer, *J. Am. Chem. Soc.*, 2012, **134**, 3972-3975; (b) T. Naota, H. Takaya and S.-I. Murahashi, *Chem. Rev.*, 1998, **98**, 2599-2660; (c) M. Pagliaro, S. Campestrini and R. Ciriminna, *Chem. Soc. Rev.*, 2005, **34**, 837-845; (d) P. B. Arockiam, C. Bruneau and P. H. Dixneuf, *Chem. Rev.*, 2012, **112**, 5879-5918; (e) T. Ishizuka, S. Ohzu and T. Kojima, *Synlett.*, 2014, **25**, 1667-1679; (f) T. Ishizuka, S. Ohzu, H. Kotani, Y. Shiota, K. Yoshizawa and T. Kojima, *Chem. Sci.*, 2014, **5**, 1429-1436; (g) S. Ohzu, T. Ishizuka, Y. Hirai, H. Jiang, M. Sakaguchi, T. Ogura, S. Fukuzumi and T. Kojima, *Chem. Sci.*, 2012, **3**, 3421-3431.

7 (a) S. L.-F. Chan, Y.-H. Kan, K.-L. Yip, J.-S. Huang and C.-M. Che, *Coord. Chem. Rev.*, 2011, **255**, 899-919; (b) W. W. Y. Lam, S.-M, Yiu, D. T. Y. Yieu, T.-C. Lau, W.-P. Yip and C.-M. Che, *Inorg. Chem.*, 2003, **42**, 8011-8018; (c) T. Kojima, Y. Hirai, T. Ishizuka, Y. Shiota, K. Yoshizawa, K. Ikemura, T. Ogura and S. Fukuzumi, *Angew. Chem. Int. Ed.*, 2010, **49**, 8449-8453; (d) M. Rodríguez, I. Romeroa, C. Sens and A. Llobet, *J. Mol. Catal. A*: *Chem.*, 2006, **282**, 215-220.

8 (a) Y.-N. Wang, K.-C. Lau, W. W. Y. Lam, W.-L. Man, C.-F. Leung and T.-C. Lau, *Inorg. Chem.*, 2009, **48**, 400-406; (b) Y. Huang, E. Vanover and R. Zhang, *Chem. Commun.*, 2010, **46**, 3776-3778.

9 (a) C.-M. Che, T.-F. Lai and K.-Y. Wong, *Inorg. Chem*., 1987, **26**, 2289-2299; (b) C.-M. Che, W.-T. Tang, W.-T. Wong and T.-F. Lai, *J. Am. Chem. Soc*., 1989, **111**, 9048-9056; (c) C. Abebrese, Y. Huang, A. Pan, Z. Yuan and R. Zhang, *J. Inorg. Biochem*., 2011, **105**, 1555-1561; (d) C.-M. Che, W.-T. Tang, W.-O. Lee, K.-Y. Wong and T.-C. Lau, *J. Chem. Soc. Dalton Trans*., 1992, 1551-1556; (e) E. L. Lebeau and T. J. Meyer, *Inorg. Chem*., 1999, **38**, 2174-2181.

10 J. T. Groves and R. Quinn, *J. Am. Chem. Soc.*, 1985, **107**, 5790-5792.

11 B. Mouzopoulou, H. Kozlowski, N. Katsaros and A. Garnier-Suillerot, *Inorg. Chem*., 2001, **40**, 6923-6929.

12 C.-M. Che, K.-Y. Wong and C.-K. Poon, *Inorg. Chem*., 1985, **24**, 1797-1800.

13 W. W. Y. Lam, W.-L. Man and T.-C. Lau, *Coord. Chem. Rev.*, 2007, **251**, 2238-2252.

14 (a) W.-C. Cheng, W.-Y. Yu, C.-K. Li and C.-M. Che, *J. Org. Chem.,* 1995, **60**, 6840-6846; (b) W. W. Y. Lam, W.-L. Man, Y.-N. Wang and T.-C. Lau, *Inorg. Chem.,* 2008, **47**, 6771-6778; (c) W. W. Y. Lam, M. F. W. Lee and T.-C. Lau, *Inorg. Chem.*, 2006, **45**, 315-321; (d) W.-L. Man, W. W. Y. Lam, W.-Y. Wong and T.-C. Lau, *J. Am. Chem. Soc*., 2006, **128**, 14669-14675; (e) C.-M. Che and K.-Y. Wong, *J. Chem. Soc. Dalton Trans.,* 1989, 2065-2067; (f) W.-L. Man, W. W. Y. Lam, S.-M. Ng, W. Y. K. Tsang and T.-C. Lau, *Chem.–Eur. J.*, 2012, **18**, 138-144; (g) D. T. Y. Yiu, M. F. W. Lee, W. W. Y. Lam and T.-C. Lau, *Inorg. Chem*., 2003, **42**, 1225-1232.

15 T. Matsuo and J. M. Mayer, *Inorg. Chem*., 2005, **44**, 2150-2158.

16 (a) D. Mauzerall and F. H. Westheimer, *J. Am. Chem. Soc.,* 1955, **77**, 2261-2264; (b) L. Stryer, *Biochemistry*, 3rd ed.; Freeman, New York, 1988, Chapter 17.

17 N. Song, M.-T. Zhang, R. A. Binstead, Z. Fang, and T. J. Meyer, *Inorg. Chem*., 2014, **53**, 4100-4105.

18 M. S. Seo, J.-H. In, S. O. Kim, N. Y. Oh, J. Hong, J. Kim, L. Que, Jr. and W. Nam, *Angew. Chem. Int. Ed*., 2004, **43**, 2417-2420.

19 (a) T. C. W. Mak, C.-M. Che and K.-Y. Wong, *J. Chem. Soc., Chem. Commun*., 1985, 986-988; (b) C.-M. Che, J.-L. Zhang, R. Zhang, J.-S. Huang, T.-S. Lai, W.-M. Tsui, X.-G. Zhou, Z.-Y. Zhou, N. Zhu and C. M. Chang, *Chem.–Eur. J.*, 2005, **11**, 7040-7053; (c) T.-S. Lai, R. Zhang, K.-K. Cheung, H.-L. Kwong and C.-M. Che, *Chem. Commun*., 1998, 1583-1584; (d) T. J. Meyer and M. H. V. Huynh, *Inorg. Chem.,* 2003, **42**, 8140-8160.

20 S. Fukuzumi, H. Kotani, Y.-M. Lee and W. Nam, *J. Am. Chem. Soc*., 2008, **130**, 15134-15142.

21 S. N. Dhuri, M. S. Seo, Y.-M. Lee, H. Hirao, Y. Wang, W. Nam and S. Shaik, *Angew. Chem. Int. Ed*., 2008, **47**, 3356-3359.

22 S. Fukuzumi, Y. Tokuda, T. Kitano, T. Okamoto and J. Otera, *J. Am. Chem. Soc.*, 1993, **115**, 8960-8968.

23 H. Yoon, Y.-M. Lee, W. Nam and S. Fukuzumi, *Chem. Commun*., 2014, **50**, 12944-12946.

24 (a) S. Fukuzumi, S. Koumitsu, K. Hironaka and T. Tanaka, *J. Am. Chem. Soc*., 1987, **109**, 305-316; (b) S. Fukuzumi, K. Ohkubo, Y. Tokuda and T. Suenobu, *J. Am. Chem. Soc.,* 2000, **122**, 4286-4294.

25 Y. J. Jeong, Y. Kang, A.-R. Han, Y.-M. Lee, H. Kotani, S. Fukuzumi and W. Nam, *Angew. Chem. Int. Ed*., 2008, **47**, 7321-7324.

26 (a) J. Y. Lee, Y.-M. Lee, H. Kotani, W. Nam and S. Fukuzumi, *Chem. Commun.*, 2009, **6**, 704-706; (b) S. Fukuzumi, N. Fujioka, H. Kotani, K. Ohkubo, Y.-M. Lee and W Nam, *J. Am. Chem. Soc*., 2009, **131**, 17127-17134; (c) Y. Han, Y.-M. Lee, M. Mariappan, S. Fukuzumi and W. Nam, *Chem. Commun*., 2010, **46**, 8160-8162; (d) S. Fukuzumi, H. Kotani, K. A. Prokop and D. P. Goldberg, *J. Am. Chem. Soc*., 2011, **133**, 1859-1869.

27 Y.-R. Luo, *Handbook of Bond Dissociation Energies in Organic Compounds*, CRC Press, New York, 2003.

28 (a) J. M. Mayer, *Acc. Chem. Res.*, 1998, **31**, 441-450; (b) A. S. Borovik, *Acc. Chem. Res*., 2005, **38**, 54-61; (c) C. R. Goldsmith, A. P. Cole and T. D. P. Stack, *J. Am. Chem. Soc.*, 2005, **127**, 9904-9912.

29 (a) T. Kojima, K. Nakayama, K. Ikemura, T. Ogura and S. Fukuzumi, *J. Am. Chem. Soc*., 2011, **133**, 11692-11700; (b) K.-B. Cho, X. Wu, Y.-M. Lee, Y. H. Kwon, S. Shaik and W. Nam, *J. Am. Chem. Soc*., 2012, **134**, 20222-20225.

30 W. L. F. Armarego and C. L. L. Chai, *Purification of Laboratory Chemicals*, 6th ed., Pergamon Press, Oxford, U.K, 2009.

31 C. V. Sastri, J. Lee, K. Oh, Y. J. Lee, J. Lee, T. A. Jackson, K. Ray, H. Hirao, W. Shin, J. A. Halfen, J. Kim, L. Que, Jr., S. Shaik and W. Nam, *Proc. Natl. Acad. Sci. USA,* 2007, **104**, 19181-19186.

32 C.-M. Che, S.-S. Kwong and C.-K. Poon, *Inorg. Chem.*, 1985, **24**, 1601-1602.

33 C. K. Mann and K. K. Barnes, *Electrochemical Reactions in Non-aqueous Systems*, Marcel Dekker, New York, 1970.

TOC

The valuable insights into the mechanism in the hydride-transfer and C-H bond activation reactions by high-valent *trans*-dioxoruthenium(VI) species is provided.